Vibrational spectroscopy of superconducting K_3C_{60} by inelastic neutron scattering

Kosmas Prassides*, John Tomkinson†, Christos Christides*, Matthew J. Rosseinsky‡, D. W. Murphy‡ & Robert C. Haddon‡

* School of Chemistry and Molecular Sciences, University of Sussex, Brighton BN1 9QJ, UK
† ISIS Science Division, Rutherford Appleton Laboratory, Didcot, OX11 0QX, UK
‡ AT&T Bell Laboratories, Murray Hill, New Jersey 07974, USA

INTERCALATION of C_{60} (buckminsterfullerene[1,2]) by alkali metals[3] leads to superconducting compounds of stoichiometry A_3C_{60} (refs 4–6) with transition temperatures T_c as high as 33 K (ref. 7). These transition temperatures are considerably higher than those for alkali-metal-intercalated graphite (<0.6 K)[8] and scale with the size of the face-centred-cubic unit cell[9]. Here we present the results of an inelastic neutron scattering study of the vibrational spectrum of the superconducting fulleride K_3C_{60} (T_c = 19.3 K). We find significant changes in the peak positions and intensities principally of the intramolecular H_g vibrational modes, both in the high-energy tangential (130–200 meV) and the low-energy radial (~50 meV) regions, compared with the vibrational spectrum of C_{60} (refs 10, 11). Our results provide strong evidence for the importance of these modes in the pairing mechanism for superconductivity.

The K_3C_{60} sample was prepared by reaction of $K_{6.6}C_{60}$ and C_{60} in a sealed evacuated pyrex tube at 250 °C for 3 days, 350 °C for 24 hours and 250 °C for 8 days[12]. Phase purity was confirmed by X-ray diffraction measurements and Rietveld refinement of high-resolution neutron powder-diffraction data. For the neutron scattering measurements, the 500-mg sample was sealed in a 9-mm-diameter fused silica tube under 0.5 atm helium. Inelastic neutron scattering (INS) measurements were done at 5 K and 30 K with the sample inside a continuous-flow 'orange' cryostat, using the time-focused crystal analyser (TFXA) spectrometer[13] at the ISIS facility, Rutherford Appleton Laboratory; a background run was recorded on an identical empty silica tube at 30 K. TFXA is an inverted-geometry white-beam spectrometer with excellent resolution, $\Delta\omega/\omega \approx 2\%$, over the entire energy transfer range, 2.5–500 meV (1 meV = 8.066 cm^{-1}). Even for primarily coherent scatterers like carbon, the instrumental characteristics of TFXA permit the use of the incoherent approximation at energy transfers >25 meV. Coherent scattering effects are important only at low-energy transfer.

The scattering law $S(Q, \omega)$ of K_3C_{60} was measured in down-scattering mode between 2.5 and 200 meV. The summed data collected at both 5 and 30 K are shown in Fig. 1. $S(Q, \omega)$ may be written as

$$S(Q,\omega)_\nu \propto (1/3)(Q^2\,\mathrm{Tr}\mathbf{B}_\nu)\exp(-Q^2\alpha_\nu)$$

$$\alpha_\nu \approx (1/5)\{\mathrm{Tr}\,\mathbf{A} + 2(\mathbf{B}_\nu : \mathbf{A}/\mathrm{Tr}\,\mathbf{B}_\nu)\}$$

where $\mathbf{A} = \Sigma_\nu \mathbf{B}_\nu$, $\mathbf{B}_\nu$ is the mean square displacement tensor of the scattering atom in mode ν and Q is the momentum transferred during scattering; other terms and conventions are defined elsewhere[14]. Carbon-60 is a molecular solid with negligible dispersion of the intramolecular phonons, and the observed peaks in $S(Q, \omega)$ correspond well to the $Q = 0$ modes observed in infrared and Raman spectroscopy. There are no selection rules in INS and hence all the vibrational modes are observed; in addition, considerations of reduced optical penetration depth in K_3C_{60}, important in Raman and infrared spectroscopy, are not relevant here. The vibrational spectrum of K_3C_{60}, like that of C_{60} (ref. 11), may be divided into two regions: (1) 2.5–25 meV, corresponding to intermolecular and K^+-C_{60}^{3-} modes with a prominent feature at 4.3 meV and a band at 14 meV with full-width at half-maximum of 7 meV; and (2) 25–200 meV, corresponding to the intramolecular modes. The vibrational modes of the molecule may be further subdivided into principally tangential motions, clustering in the high-energy region (110–200 meV) and radial (buckling) motions in the low-energy region (25–110 meV). The symmetry of most of the buckling modes up to 110 meV may be inferred by comparison with C_{60}; there are well-resolved bands at 33 ($H_g^{(1)}$), 44 (T_{2u}, G_u), 49 (H_u), 60 (G_g), 68 (T_{1u}), 71 (T_{1u}), 82 and 87 meV ($H_g^{(3)}$), and a broad band with peaks at 93 and 97 meV ($H_g^{(4)}$). The high-energy region does not show sharp well-defined features and divides roughly into three parts with pronounced cut-offs in intensity: 110–135, 135–170 and 170–200 meV.

Insight into the changes in the intramolecular bonding of C_{60} on intercalation, and the relevance of the various vibrational modes to the mechanism of superconductivity, can be obtained by comparing the low-temperature INS spectra of K_3C_{60} and C_{60}. The striking difference between the two systems is the redistribution of intensity that occurs between the radial and tangential modes. Carbon-60 has intense features up to ~110 meV, followed by many weaker and broader bands up to

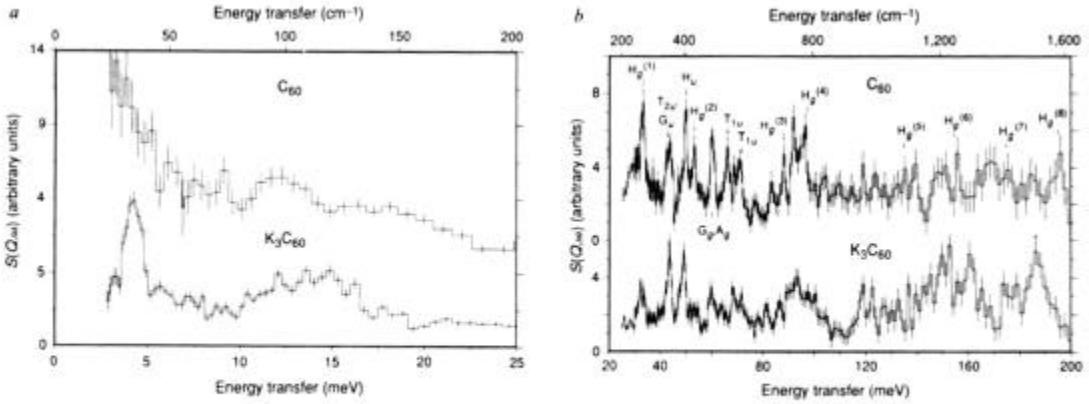

FIG. 1 Inelastic neutron scattering spectra in the energy regions (*a*) 0–25 meV and (*b*) 25–200 meV of C_{60} at 20 K (top) and K_3C_{60} (bottom); the K_3C_{60} data were collected at 5 K and 30 K and summed. The instrumental resolution is $\Delta\omega/\omega \approx 2\%$, corresponding to decreased resolution at high energy transfers. Some mode assignments in the icosahedral point group (I_h) are shown.

200 meV. In this respect, it resembles graphite which shows the same distribution of intensity between modes involving out-of-plane and in-plane motion[15]. In K_3C_{60}, on the other hand, the high-energy region is intense. The physical reasons behind these changes in intensity are not clear, but they may reflect increased mixing between radial and tangential modes. One possible mechanism involves the strengthening of interaction force-constants. The effect of this would be to switch intensity between the interacting vibrations, without necessarily changing their energy very much.

Theoretical treatments of superconductivity in A_3C_{60} have considered purely electronically induced[16] as well as phonon-induced pairing, involving either low-frequency (~10–20 meV) K^+–C_{60}^{3-} optic modes[17] or the high-energy intramolecular modes[18,19]. In addition, the symmetry considerations for the intramolecular coupling models allow only A_g and H_g phonons to couple to the t_{1u} conduction electrons. Schluter *et al.*[18] find coupling strength distributed over both the low-frequency radial modes and the high-frequency tangential modes, whereas Varma *et al.*[19] find that the purely tangential $H_g^{(7)}$ and $H_g^{(8)}$ modes at 177 and 196 meV dominate the pairing mechanism. Strong electron–phonon coupling will produce substantial broadening and softening (~10–20%) of the affected modes. Raman spectroscopy is sensitive to the A_g and H_g modes with both A_g and all eight H_g modes evident for C_{60}. Room-temperature Raman spectra[20] of A_3C_{60} thin films show only two A_g modes and the lowest-frequency $H_g^{(1)}$ mode, the absence of the other modes being attributed either to decreased optical penetration depth or lifetime broadening of the spectral function due to electron–phonon coupling.

The INS data confirm the electron–phonon coupling to at least some of the H_g modes. Indeed the most remarkable difference between the K_3C_{60} and C_{60} spectra is the disappearance of the $H_g^{(2)}$ and $H_g^{(8)}$ modes at 54 and 196 meV, consistent with strong electron–phonon coupling. This is an important difference from alkali-intercalated graphite, where the corresponding buckling $H_g^{(2)}$ mode does not couple to the π-electrons because of symmetry considerations. Radial $H_g^{(1)}$, $H_g^{(3)}$ and $H_g^{(4)}$ modes are present in K_3C_{60} at 33, 87 and 97 meV and show only slightly reduced intensities and increased broadening, consistent with minor contributions to the electron–phonon coupling strength. A definitive statement about the effect of intercalation on the $H_g^{(5-7)}$ modes at 136, 155 and 177 meV in C_{60} is difficult because they are weak, but there are significant changes in the spectra of K_3C_{60} in these regions. Although definitive peak assignments must await detailed modelling, it is tempting to assign the broad feature in K_3C_{60} at 186 meV to $H_g^{(8)}$, corresponding to a softening of ~6%. The differences between C_{60} and K_3C_{60} in the 10–20 meV region may be due to K^+–C_{60}^{3-} optic modes.

We have also recorded the INS spectra of K_3C_{60} above (30 K) and below (5 K) the superconducting transition temperature. There is only modest evidence for changes in the intensity of the intramolecular modes in the 135–170 and 170–200 meV regions, as the sample goes through T_c. A decrease in intensity is, however, observed between 30 and 5 K at 4.2 meV; there is also some indication that this is accompanied by an increased broadening. Note that the scattering in this energy range is completely coherent, and we are cutting through a phonon, probably acoustic, branch. These effects may be caused by an as yet undetected structural anomaly at or above T_c, or arise because the phonon energy is close to the superconducting energy gap ($2\Delta \approx 40$ K (ref. 21)). We note that the presence of soft acoustic phonons is well documented in the case of A15-structure superconducting materials[22].

Our data provide strong evidence for the presence of electron–phonon coupling to H_g modes of K_3C_{60}, as predicted by intramolecular phonon theories[18,19]. Higher-resolution data and detailed mode assignments are needed for a more complete picture, particularly the location of the softened H_g modes in K_3C_{60}, identification of optic modes and the nature of the near-gap scattering law below T_c. □

Received 8 November; accepted 20 November 1991.

1. Kroto, H. W., Heath, J. R., O'Brien, S. C. & Smalley, R. E. *Nature* **318**, 162–164 (1985).
2. Krätschmer, W., Lamb, L. D., Fostiropoulos, K. & Huffman, D. R. *Nature* **347**, 354–358 (1990).
3. Haddon, R. C. *et al. Nature* **350**, 320–322 (1991).
4. Hebard, A. F. *et al. Nature* **318**, 600–601 (1991).
5. Rosseinsky, M. J. *et al. Phys. Rev. Lett.* **66**, 2830–2832 (1991).
6. Holczer, K. *et al. Science* **252**, 1154–1157 (1991).
7. Tanigaki, K. *et al. Nature* **352**, 222–223 (1991).
8. Hannay, N. B. *et al. Phys. Rev. Lett.* **14**, 225–226 (1965).
9. Fleming, R. M. *et al. Nature* **352**, 787–788 (1991).
10. Cappelletti, R. L. *et al. Phys. Rev. Lett.* **66**, 3261–3264 (1991).
11. Prassides, K. *et al. Chem. Phys. Lett.* (in the press).
12. McCauley, J. P. Jr *et al. J. Am. chem. Soc.* **113**, 8537–8538 (1991).
13. Penfold, J. & Tomkinson, J. *Rutherford Appleton Lab. Internal Rep.* RAL-86-019 (1986).
14. Tomkinson, J., Warner, M. & Taylor, A. D. *Molec. Phys.* **51**, 381–392 (1984).
15. Hannon, A. C. & Tomkinson, J. *Rutherford Appleton Lab. ISIS Ann. Rep.* A138 (1989).
16. Chakravarty, S. & Kivelson, S. *Europhys. Lett.* **16**, 751–756 (1991).
17. Zhang, F. C., Ogata, M. & Rice, T. M. *Phys. Rev. Lett.* (submitted).
18. Schluter, M., Lannoo, M., Needels, M., Baraff, G. A. & Tomanek, D. *Phys. Rev. Lett.* (submitted).
19. Varma, C. M., Zaanen, J. & Raghavachari, K. *Science* **254**, 989–992 (1991).
20. Duclos, S. J., Haddon, R. C., Glarum, S., Hebard, A. F. & Lyons, K. B. *Science* (in the press).
21. Tycko, R. *et al. Phys. Rev. Lett.* (submitted).
22. Shirane, G., Axe, J. D. & Birgeneau, R. J. *Solid State Commun.* **9**, 397–399 (1971).

ACKNOWLEDGEMENTS. We acknowledge J. White and M. Schluter for discussions. We thank R. Fleming for recording the X-ray and R. Ibberson and W. David for the high-resolution neutron diffraction profile. We thank SERC for financial support (K.P.) and for access to ISIS.

Layered magnetic structure of a metal cluster ion

D. Gatteschi*‡, L. Pardi*, A. L. Barra*, A. Müller†‡ & J. Döring†

* Dipartimento di Chimica, Università di Firenze, Italy
† Fakultät für Chemie, Universität Bielefeld, Germany

THE ability of molecular materials to perform many of the optical, electronic and magnetic functions traditionally associated with extended two- and three-dimensional inorganic solids[1,2] has given rise to intensive research on molecular electronics[3,4]. In the course of investigating the properties of a class of anionic metal clusters based on the vanadium oxide systems[5–8], which bear analogy with those of bulk solid materials[6], we have encountered unusual magnetic behaviour in a finite molecular system. A cluster containing 15 paramagnetic vanadium atoms consists of three distinct layers in each of which the magnetization shows a distinct temperature dependence. Analogous behaviour in bulk systems can be found in magnetic multilayers[9] and also in copper oxide superconductors, where copper layers with strong antiferromagnetic coupling are separated by layers of rare-earth ions in which the coupling is very weak[10]. The behaviour of this cluster suggests the possibility of applications for molecular-scale switching.

$K_6[V_{15}^{IV}As_6O_{42}(H_2O)] \cdot 8\,H_2O$ was prepared as described previously[11]. It has a crystallographically imposed trigonal symmetry[11] (space group $R\bar{3}c$, No. 167), as shown in Fig. 1*a*. The overall structure is quasispherical, with three sets of (non-equivalent) vanadium atoms, V_1, V_2 and V_3. V_1 and V_2 define two nonplanar hexagons separated by a triangle of V_3 centres (Fig. 1*b*). This 'layer structure' has paramount importance in determining the magnetic properties to be described below.

Figure 2 shows the temperature dependence of the effective magnetic moment per formula unit, $\mu_{eff} \propto (\chi T)^{1/2}$, where T is temperature and χ is magnetic susceptibility of $K_6[V_{15}As_6O_{42}(H_2O)] \cdot 8\,H_2O$ in the range of 5–300 K, measured with a Faraday apparatus[12]. The room-temperature value, 4.05 μ_B, is much lower than expected for 15 uncoupled

‡ To whom correspondence should be addressed.